High-valent Diphenylacetylene Complexes of Tungsten†

Alastair J. Nielson,*[a] Peter D. W. Boyd,[a] George R. Clark,[a] Patricia A. Hunt,[a] Michael B. Hursthouse,[b] James B. Metson,[a] Clifton E. F. Rickard[a] and Peter A. Schwerdtfeger[a]

[a] *Department of Chemistry, University of Auckland, Private Bag 92019, Auckland, New Zealand*

[b] *School of Chemistry and Applied Chemistry, University of Wales College of Cardiff, PO Box 912, Cardiff CF1 3TPB, UK*

The W(4f$_7$) binding energy of [{$WCl_4(PhC_2Ph)$}$_2$] **1** obtained by X-ray photoelectron spectroscopy is similar to that of [{$WCl_4(NPh)$}$_2$] and is consistent with a d^0 tungsten(VI) formulation. The reaction of complex **1** and [NEt_4][$WCl_5(PhC_2Ph)$] **2** with NaOH–EtOH gave *cis*-stilbene, indicating considerable electron transfer from the metal to the co-ordinated alkyne. Reduction of complex **1** with 2 equivalents of sodium–mercury amalgam in the presence of phosphines gave the complexes [$WCl_3(PhC_2Ph)L_2$] (L = PMe_3, PMe_2Ph or $PMePh_2$) with magnetic moments and W(4f$_7$) binding energies similar to those of the d^1 tungsten(V) organoimido complex [$WCl_3(NPh)(PMe_3)_2$]. Decomposition of the alkyne complexes with NaOH–EtOH again gave *cis*-stilbene. The crystal structure of [$WCl_3(PhC_2Ph)(PMe_3)_2$] **3** has been determined. The W–Cl bond *trans* to the alkyne ligand is long [2.479(3) Å], and the W–C bond lengths [2.011(13) and 2.038(12) Å] indicate a four-electron-donor alkyne ligand. The geometry is similar to that of [$WCl_3(NPh)(PMe_3)_2$]. Reduction of [{$WCl_4(PhC_2Ph)$}$_2$] using 4 equivalents of sodium–mercury amalgam in the presence of phosphines gave the complexes [$WCl_2(PhC_2Ph)L_3$] (L = PMe_3 or PMe_2Ph) which again produced *cis*-stilbene on decomposition with NaOH–EtOH. The acetylenic carbon resonance at δ 223.15 in the ^{13}C-{^1H} NMR spectrum of [$WCl_2(PhC_2Ph)(PMe_3)_3$] **6** is also indicative of a four-electron-donor alkyne ligand. Its W(4f$_7$) binding energy is similar to [$WCl_2(NPh)(PMe_3)_3$] and is consistent with tungsten(IV). A crystal structure of complex **6** shows a similar ligand geometry to [WCl_2-$(NPh)(PMe_3)_3$], and the W–C bond lengths [2.019(11) and 2.006(11) Å] indicate a four-electron-donor alkyne ligand. Hartree–Fock and scattered wave Xα calculations have been performed on the model complexes [$WCl_5(HC_2H)$]$^-$ **8**, [$WCl_3(HC_2H)(PH_3)_2$] **9** and [$WCl_2(HC_2H)(PH_3)_3$] **10**. Molecular orbital and population analyses indicated that the acetylene–tungsten bond in each involves $W(5d_\pi) \longrightarrow HC_2H(\pi^*)$ back donation as well as $HC_2H(\pi) \longrightarrow W(5d_\sigma)$ and $HC_2H(\pi_\perp) \longrightarrow W(5d_\pi)$ forward donation, consistent with a four-electron-donor alkyne formalism. Electron withdrawal from the tungsten to the more electronegative Cl ligand in complexes **8** and **9** is minimised by rotation of the alkyne away from the meridional vectors. In complex **10** the $HC_2H(\pi_\perp) \longrightarrow W(5d_\pi)$ donation and phosphine contributions compensate and no rotation is observed. The total d atomic orbital population of complex **8** is close to that of WCl_6, and populations of complexes **9** and **10** step up linearly from this. The computational results support the experimental evidence that [{$WCl_4(PhC_2Ph)$}$_2$] **1**, [$WCl_3(PhC_2Ph)(PMe_3)_2$] **3** and [$WCl_2(PhC_2Ph)(PMe_3)_3$] **6** are complexes of tungsten-(VI), -(V) and -(IV) respectively.

Alkyne complexes of the earlier transition metals are well known and have been investigated in detail.[1] Recent work in this field has shown that metal-to-ligand interactions may be sufficiently strong to change the formal oxidation state of the metal and reduce the alkyne ligand.[2] The extent of reduction is such that alkyne complexes have been used as a source of 1,2-alkene dianions in organic synthesis.[3] The alkyne ligand is generally considered to be π bound to the transition metal in a manner similar to the Dewar–Chatt–Duncanson model for olefins (a_1 and b_1 interactions in the local C_{2v} point group), but with the additional possibility of a $\pi_\perp$ alkyne interaction with the metal [a_2 and b_2 interactions in the local C_{2v} point group,[1] (Fig. 1)].

Formally, an alkyne ligand is a two-electron donor if donation is from the $\pi_\parallel$ (acetylene π-parallel) frontier orbital only. If, in addition, strong donation from the $\pi_\perp$ (acetylene π-perpendicular) frontier orbitals to metal atomic orbitals (AOs) occurs as well, then the alkyne is formally a four-electron donor.[1] This description, however, is exclusive of any back donation from the metal to the alkyne, and therefore may be slightly misleading since this component of the bonding is also important if the formal oxidation state of the central metal is discussed.

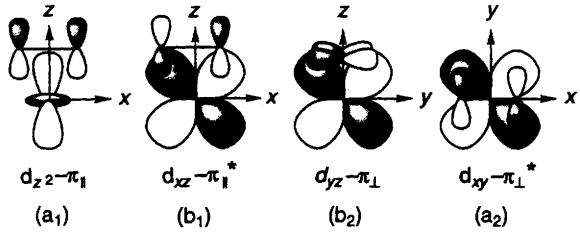

Fig. 1 Frontier MOs for a metal–alkyne complex

In this paper we report experimental and theoretical evidence for the stabilisation of high oxidation states by alkyne ligands. In particular, we show that diphenylacetylene complexes of tungsten exhibit properties and chemistry similar to that found for complexes considered to contain the +6, +5 and +4 oxidation states of this metal. A preliminary account of some of this work has appeared.[4]

† *Supplementary data available:* see Instructions for Authors, *J. Chem. Soc., Dalton Trans.*, 1995, Issue 1, pp. xxv–xxx.

Non-SI units employed: $\mu_B = 9.27 \times 10^{-24}$ J T^{-1}, eV ≈ 1.60×10^{-19} J.

Results and Discussion

Synthetic Studies.—The alkyne complex $[\{WCl_4(PhC_2Ph)\}_2]$ **1** is easily prepared from WCl_6 and diphenylacetylene as a dark red-brown solid which is very sensitive to air and moisture.[5] It is poorly soluble in non-co-ordinating solvents, but forms 1:1 adducts in tetrahydrofuran (thf), diethyl ether and MeCN which are apparently stable only in solution. Complex **1** reacts with $[NEt_4]Cl$ in CH_2Cl_2 to give a dark red solution, but subsequent removal of the solvent leaves a solid which fails to redissolve. A 2:1 solution of $[NEt_4]Cl$ and $[\{WCl_4(PhC_2Ph)\}_2]$ in CD_2Cl_2 gives a single set of NMR resonances suggesting the formation of $[NEt_4][WCl_5(PhC_2Ph)]$ **2**. The ^{13}C-$\{^1H\}$ NMR spectrum of complex **2** shows the acetylenic carbons as a single resonance at δ 270.7 which is characteristic of a four-electron-donor alkyne ligand in an electron-deficient alkyne complex.[6] In CD_3CN, where the expected complex is $[WCl_4(PhC_2Ph)(CD_3CN)]$, the ^{13}C acetylenic resonance occurs at δ 268.4.

In order to make an experimental estimation of the formal oxidation state of tungsten in complex **1** we have determined the $W(4f_{\frac{7}{2}})$ binding energy by X-ray photoelectron spectroscopy (XPS). Its value of 35.1 eV (Table 1) falls within the range for complexes considered to be tungsten(VI),[7] and is close to that measured from the structurally similar d^0 tungsten(VI) organoimido complex $[\{WCl_4(NPh)\}_2]$ (35.8 eV). High oxidation-state character in complexes **1** and **2** is further emphasised by reaction with aqueous sodium hydroxide in ethanol whereby *cis*-stilbene is produced, indicating that the co-ordinated alkyne was in a substantially reduced state.

Reductions of complex **1** in benzene with 1 equivalent of sodium–mercury amalgam in the presence of phosphine ligands afforded the complexes $[WCl_3(PhC_2Ph)L_2]$ (L = PMe_3, PMe_2Ph or $PMePh_2$) obtained as crystalline orange air-stable solids (Table 2). The complexes exhibit a band in the IR spectrum at about 1660 cm^{-1} attributable to ν(C≡C) of the diphenylacetylene ligand. There are three W–Cl stretching bands in the far IR which are consistent with a *mer* arrangement of metal trichlorides[8,9] (Table 2). These complexes exhibit solid-state and solution (Evans' method) magnetic moments consistent with tungsten(V) species (Table 2). For example, $[WCl_3(PhC_2Ph)(PMe_3)_2]$ **3** shows a solution magnetic moment μ_{eff} = 1.51 μ_B similar to that found for d^1 tungsten oxo complexes[10] and the d^1 tungsten(V) organoimido complex $[WCl_3(NPh)(PMe_3)_2]$ (μ_{eff} = 1.43 μ_B).[9] Further evidence showing that complex **3** is formally tungsten(V) is obtained from the EPR spectrum, where the *g* value is 1.905 (A_P 30 G), which is similar to that found for $[WCl_3(NPh)(PMe_3)_2]$ (*g* value 1.897 and A_P 29 G).[9]

X-Ray photoelectron spectroscopy was again employed to obtain the $W(4f_{\frac{7}{2}})$ binding energies of $[WCl_3(PhC_2Ph)(PMe_3)_2]$ **3** and $[WCl_3(PhC_2Ph)(PMe_2Ph)_2]$ **4**. (Table 1) The values measured (33.6 eV for both complexes) are similar to that obtained for the tungsten(V) organoimido complex $[WCl_3(NPh)(PMe_3)_2]$ (34.0 eV) and the recently determined cyano complex $[NBu_4]_3[W(CN)_8]$[11] (33.6 eV). Decomposition of complexes **3** and **4** by aqueous sodium hydroxide in ethanol again led exclusively to *cis*-stilbene.

We have determined the single-crystal structure of $[WCl_3(PhC_2Ph)(PMe_3)_2]$ **3** (Fig. 2). The tungsten atom is in a distorted octahedral array, comprising *trans*-phosphine ligands, the acetylene function, and a meridional arrangement of the three chloro groups. This ligand arrangement is similar to that found for the d^1 organoimido complex $[WCl_3(NPh)(PMe_3)_2]$[9] and the d^1 oxo complex $[WCl_3(O)(PEt_3)_2]$.[12] Atomic co-ordinates for complex **3** are listed in Table 3 and selected bond lengths and angles in Table 4, where they are compared to data obtained for $[WCl_3(NPh)(PMe_3)_2]$.[9] In both complexes the phosphine and chloro ligands lying in the equatorial plane are repelled away from the PhC_2Ph or NPh ligands. The W–Cl bond *trans* to the PhC_2Ph or NPh ligands are considerably

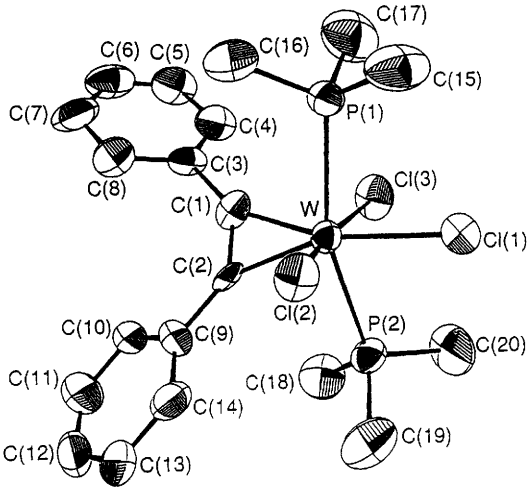

Fig. 2 Molecular structure of complex **3**. Atoms are depicted as 50% probability surfaces. Hydrogen atoms have been omitted

Table 1 $W(4f_{\frac{7}{2}})$ binding energy for several tungsten complexes

Complex	Binding energy/eV	Formal oxidation state
$[\{WCl_4(PhC_2Ph)\}_2]$ **1**	35.1	+6
$[\{WCl_4(NPh)\}_2]$	35.8	+6
$[WCl_3(PhC_2Ph)(PMe_3)_2]$ **3**	33.6	+5
$[WCl_3(NPh)(PMe_3)_2]$	34.0	+5
$[WCl_3(PhC_2Ph)(PMe_2Ph)_2]$ **4**	33.6	+5
$[WCl_2(PhC_2Ph)(PMe_3)_3]$ **6**	32.7	+4
$[WCl_2(NPh)(PMe_3)_3]$	32.5	+4

Table 2 Physical data

Complex	Colour	Analysis[a] (%) C	H	P	Magnetic susceptibility[b] μ_B	IR $\tilde{\nu}$/cm^{-1} ν(W–Cl)
3 $[WCl_3(PhC_2Ph)(PMe_3)_2]$	Orange	39.0 (38.7)	4.5 (4.6)	10.0 (10.0)	1.45 (1.51)	310, 290, 260
4 $[WCl_3(PhC_2Ph)(PMe_2Ph)_2]$	Orange	48.8 (48.4)	4.3 (4.3)	8.6 (8.3)	1.35 (1.61)	310, 290, 265
5 $[WCl_3(PhC_2Ph)(PMePh_2)_2]$	Orange	55.5 (55.3)	4.3 (4.2)	6.8 (7.1)	1.59 (1.63)	310, 290, 265
6 $[WCl_2(PhC_2Ph)(PMe_3)_3]$	Green	41.0 (41.8)	5.5 (5.6)	13.8 (14.1)	—	278, 235
7 $[WCl_2(PhC_2Ph)(PMe_2Ph)_2]$	Green	53.9 (53.9)	5.0 (5.1)	10.9 (11.0)	—	290, 260

[a] Calculated values given in parentheses. [b] Solid-state determinations; solution determinations are in parentheses.

Table 3 Atomic coordinates for complex **3**

Atom	*x*	*y*	*z*
W	0.167 22(5)	0.002 15(5)	0.138 69(2)
Cl(1)	0.108 7(5)	0.173 2(3)	0.197 14(14)
Cl(2)	−0.078 1(4)	−0.071 3(3)	0.174 33(12)
Cl(3)	0.394 0(4)	0.119 1(3)	0.111 41(16)
P(1)	−0.014 9(4)	0.117 3(3)	0.076 50(13)
P(2)	0.348 3(5)	−0.049 2(3)	0.216 24(13)
C(1)	0.210 3(14)	−0.101 1(11)	0.075 6(5)
C(2)	0.206 1(13)	−0.169 8(10)	0.117 0(4)
C(3)	0.232 4(15)	−0.119 8(11)	0.018 5(4)
C(4)	0.332 2(19)	−0.042 9(13)	−0.010 8(5)
C(5)	0.359(2)	−0.065 7(15)	−0.065 2(6)
C(6)	0.290(2)	−0.155 9(17)	−0.088 1(7)
C(7)	0.189(2)	−0.234 0(16)	−0.060 7(6)
C(8)	0.165 7(19)	−0.215 5(13)	−0.007 9(6)
C(9)	0.223 0(14)	−0.295 5(10)	0.131 3(5)
C(10)	0.313 2(19)	−0.370 4(11)	0.101 3(5)
C(11)	0.331(2)	−0.492 0(14)	0.114 3(6)
C(12)	0.246(2)	−0.534 7(12)	0.157 2(7)
C(13)	0.154(2)	−0.462 0(12)	0.188 4(6)
C(14)	0.144 9(17)	−0.343 6(12)	0.174 5(5)
C(15)	−0.159(2)	0.211 4(15)	0.107 0(6)
C(16)	−0.134(2)	0.025 9(14)	0.033 3(7)
C(17)	0.083(2)	0.218 3(15)	0.032 6(7)
C(18)	0.518 6(19)	−0.140 2(14)	0.198 8(7)
C(19)	0.261 3(20)	−0.126 0(17)	0.271 6(6)
C(20)	0.447(3)	0.077 2(14)	0.243 8(8)

Table 4 Selected bond lengths (Å) and angles (°) for $[WCl_3(PhC_2Ph)(PMe_3)_2]$ **3** and $[WCl_3(NPh)(PMe_3)_2]$

	$[WCl_3(PhC_2Ph)(PMe_3)_2]$	$[WCl_3(NPh)(PMe_3)_2]$*
Cl(1)–W	2.479(3)	2.470(2)
Cl(2)–W	2.393(3)	2.387(2)
Cl(3)–W	2.413(3)	2.390(2)
P(1)–W	2.549(3)	2.531(2)
P(2)–W	2.552(3)	2.543(2)
C(1)–W	2.011(13)	
C(2)–W	2.038(12)	
C(1)–C(2)	1.304(15)	
Cl(2)–W–Cl(1)	82.6(1)	85.0(1)
Cl(3)–W–Cl(1)	84.5(1)	85.3(1)
Cl(3)–W–Cl(2)	166.7(1)	170.2(1)
P(1)–W–Cl(1)	81.8(1)	83.0(1)
P(1)–W–Cl(2)	84.0(1)	89.3(1)
P(1)–W–Cl(3)	90.9(1)	91.3(1)
P(2)–W–Cl(1)	80.3(1)	98.9(1)
P(2)–W–Cl(2)	98.1(1)	88.8(1)
P(2)–W–Cl(3)	82.9(1)	89.5(1)
P(2)–W–P(1)	161.6(1)	172.8(1)
C(1)–W–Cl(1)	163.9(4)	
C(1)–W–Cl(2)	104.8(3)	
C(1)–W–Cl(3)	86.9(3)	
C(2)–W–Cl(1)	158.5(3)	
C(2)–W–Cl(2)	84.9(3)	
C(2)–W–Cl(3)	108.3(3)	
C(2)–W–C(1)	37.64(4)	
C(2)–C(1)–W	72.3(7)	
C(1)–C(2)–W	70.1(8)	
C(3)–C(1)–C(2)	135.2(12)	
C(9)–C(2)–C(1)	140.1(11)	

* Taken from ref. 9(*a*).

lengthened in comparison with the other W–Cl bonds {for complex **3** W–Cl(1) 2.479(3), W–Cl(2) 2.393(3) Å; for $[WCl_3(NPh)(PMe_3)_2]$[9] W–Cl(1) 2.470(2), W–Cl(2) 2.387(2) Å} indicative of a strong *trans* influence. The W–C(1), W–C(2) and C≡C bond lengths found for **3** [2.011(13), 2.038(12) and 1.304(15) Å] are not significantly different to those found for $[\{WCl_4(Me_3SiC_2SiMe_3)\}_2]$[13] and $[PPh_4][WCl_5(PhC_2H)]\cdot CH_2Cl_2$,[14] which are analogues of complexes **1** and **2**. The orientation of the PhC_2Ph ligand in **3** is such that the C–C bond nearly bisects the P(1)–P(2) and Cl(2)–Cl(3) vectors (C–C bond bisection angles 56 and 44°). This feature is also found in $[\{WCl_4(Me_3SiC_2SiMe_3)\}_2]$ and $[PPh_4][WCl_5(PhC_2H)]\cdot CH_2Cl_2$, which are formally tungsten(VI), but the C–C bond more equally bisects the two Cl–Cl vectors in these examples. The current features shown by complex **3** are also not significantly different from those exhibited by $[WCl_3(PhC_2Ph)(PMe_2Ph)_2]$ **4**.[4]

When a mixture of PMe_3 and $[\{WCl_4(PhC_2Ph)\}_2]$ **1** is reduced using 4 equivalents of sodium–mercury amalgam the green, air-stable complex $[WCl_2(PhC_2Ph)(PMe_3)_3]$ **6** is obtained. With PMe_2Ph, the reduction gives a medium yield of $[WCl_2(PhC_2Ph)(PMe_2Ph)_3]$ **7** while the reaction apparently fails when $PMePh_2$ is used. Complexes **6** and **7** are obtained in better yield by reduction of the respective $[WCl_3(PhC_2Ph)L_2]$ complexes with 1 equivalent of sodium–mercury amalgam and the appropriate phosphine.†

Infrared spectra of complexes **6** and **7** each show two W–Cl stretches consistent with *cis*-oriented chloro ligands. Complex **7** apparently decomposes in solution so NMR data only for **6** were obtained. The ^1H NMR spectrum shows the PMe_3 ligand methyl resonance as a 2:1 triplet and doublet consistent with a *mer*-phosphine configuration. In the $^{13}C\text{-}\{^1H\}$ NMR spectrum the phosphine carbon resonances show a doublet and triplet and the acetylenic carbons are a ^{31}P-coupled doublet of triplets [$^2J(CP)_{cis}$ 6.91, $^2J(CP)_{trans}$ 15.91 Hz]. The position of this multiplet (δ 223.15) indicates a four-electron-donor alkyne ligand[1] which is the requirement for an overall 18-electron count for the complex. An XPS spectrum of complex **6** (Table 1) shows a W($4f_{\frac{7}{2}}$) binding energy of 32.7 eV which is similar to that obtained for the d^2 organoimido complex $[WCl_2(NPh)(PMe_3)_3]$[16]. These values lie within the range considered to be tungsten(IV).‡[7] Complex **6** appears to be indefinitely air-stable, but an XPS spectrum of a sample aged in air for several months shows a small amount of surface oxidation product containing tungsten(VI). Decomposition of complexes **6** and **7** by aqueous sodium hydroxide in ethanol again yields *cis*-stilbene exclusively.

A crystal-structure determination of $[WCl_2(PhC_2Ph)(PMe_3)_3]$ **6** shows a distorted octahedral geometry with a meridional arrangement of phosphine ligands, all of which lie *cis* to the diphenylacetylene ligand (Fig. 3). Chloro ligands lie *trans* to the diphenylacetylene ligand and *trans* to one phosphine ligand. The complex has a similar geometry to the tungsten(IV) organoimido complex $[WCl_2(NPh)(PMe_3)_3]$[16] and the oxo complexes $[WBr_2(O)L_3]$ (L = PMe_2Ph or $PMePh_2$).[17] Atomic coordinates for complex **6** are listed in Table 5, and bond lengths and angles are compared with those found for $[WCl_2(NPh)(PMe_3)_3]$[16] in Table 6. In both molecules the equatorial chloro and phosphine ligands are repelled away from the diphenylacetylene or phenylimido ligand [for complex **6**, P(2)–W–P(1) 153.8(1) and P(3)–W–C1(2) 163.1(1)°]. The bond length for the chloro ligand *trans* to the alkyne is significantly longer than the equatorial chloro ligand [W–Cl 2.500(3) and 2.465(3) Å respectively] again indicating a significant *trans* influence. The W–Cl(1) bond is similar in length to that found for the phenylimido complex [W–Cl(1) 2.501(1) Å] but in this complex the W–Cl bond length for the equatorial chloro ligand is only slightly shorter [2.491(1) Å]. The W–C(1), W–C(2) and C(1)–C(2) bond lengths in **6**

† Initial results of studies using $[\{MoCl_4(PhC_2Ph)\}_x]$[15] show that $[MoCl_2(PhC_2Ph)(PMe_3)_3]$ can be prepared by reduction using 2 equivalents of sodium–mercury amalgam per molybdenum in the presence of PMe_3.

‡ A more extensive XPS study of tungsten complexes in a variety of different oxidation states is presently being undertaken to verify these observations.

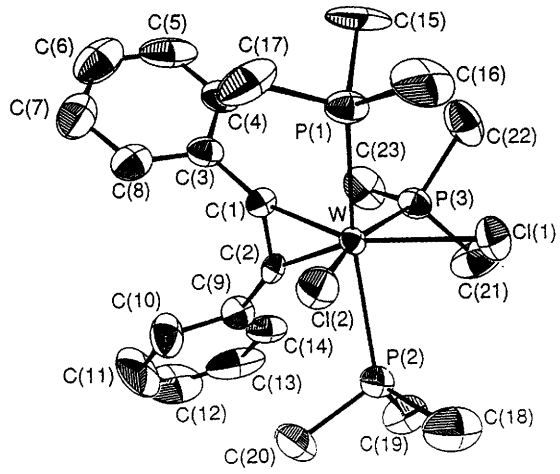

Fig. 3 Molecular structure of complex **6**. Atoms are depicted as 50% probability surfaces. Hydrogen atoms have been omitted

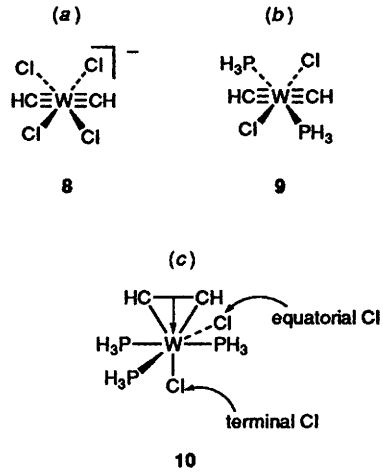

Fig. 4 Model complexes (*a*) $[WCl_5(HC_2H)]^-$ **8**, (*b*) $[WCl_3(HC_2H)(PH_3)_2]$ **9** and (*c*) $[WCl_2(HC_2H)(PH_3)_3]$ **10**

Table 5 Atomic coordinates for complex **6**

Atom	*x*	*y*	*z*
W	0.269 38(3)	0.182 12(5)	0.101 38(3)
Cl(1)	0.364 84(19)	0.307 9(4)	0.213 82(19)
Cl(2)	0.211 8(2)	0.075 9(4)	0.207 86(19)
P(1)	0.372 6(2)	−0.005 7(4)	0.147 87(19)
P(2)	0.165 4(2)	0.359 3(4)	0.122 7(2)
P(3)	0.354 5(2)	0.320 7(4)	0.029 8(2)
C(1)	0.236 6(7)	0.058 4(12)	0.004 4(6)
C(2)	0.183 4(7)	0.160 5(11)	−0.003 7(6)
C(3)	0.242 9(8)	−0.056 7(14)	−0.046 3(7)
C(4)	0.304 9(8)	−0.071 8(15)	−0.086 9(7)
C(5)	0.307 6(11)	−0.184(2)	−0.136 9(9)
C(6)	0.247 3(14)	−0.280 8(17)	−0.145 5(10)
C(7)	0.183 9(11)	−0.267 3(16)	−0.105 8(10)
C(8)	0.183 1(9)	−0.156 3(14)	−0.055 9(8)
C(9)	0.111 1(7)	0.199 8(14)	−0.067 7(7)
C(10)	0.041 0(9)	0.113 0(17)	−0.085 4(10)
C(11)	−0.027 8(11)	0.147(2)	−0.148 5(14)
C(12)	−0.027 6(14)	0.260(3)	−0.191 8(13)
C(13)	0.040 4(13)	0.345(2)	−0.174 2(9)
C(14)	0.108 1(8)	0.311 8(17)	−0.113 0(7)
C(15)	0.459 7(10)	−0.045(2)	0.102 3(11)
C(16)	0.426 7(10)	−0.002 0(18)	0.255 0(8)
C(17)	0.323 6(11)	−0.171 1(16)	0.143 5(10)
C(18)	0.182 7(10)	0.420 0(19)	0.227 8(9)
C(19)	0.147 2(10)	0.519 0(16)	0.067 2(10)
C(20)	0.058 6(8)	0.294 6(16)	0.105 5(9)
C(21)	0.350 8(13)	0.502 0(15)	0.042 0(13)
C(22)	0.467 0(8)	0.290 0(19)	0.057 1(10)
C(23)	0.335 0(10)	0.303(2)	−0.081 0(8)

Table 6 Selected bond lengths (Å) and angles (°) for $[WCl_2(PhC_2Ph)(PMe_3)_3]$ **6** and $[WCl_2(NPh)(PMe_3)_3]$

	$[WCl_2(PhC_2Ph)(PMe_3)_3]$	$[WCl_2(NPh)(PMe_3)_3]$*
Cl(1)–W	2.500(3)	2.501(1)
Cl(2)–W	2.465(3)	2.491(1)
P(1)–W	2.529(3)	2.497(1)
P(2)–W	2.549(3)	2.483(1)
P(3)–W	2.481(3)	2.453(1)
C(1)–W	2.019(11)	
C(2)–W	2.006(11)	
C(1)–C(2)	1.330(16)	
Cl(2)–W–Cl(1)	86.9(1)	84.3(1)
P(1)–W–Cl(1)	82.9(1)	90.5(1)
P(1)–W–Cl(2)	78.8(1)	82.3(1)
P(2)–W–Cl(1)	82.7(1)	91.4(1)
P(2)–W–Cl(2)	78.6(1)	86.2(1)
P(2)–W–P(1)	153.8(1)	168.1(1)
P(3)–W–Cl(1)	76.2(1)	77.2(1)
P(3)–W–Cl(2)	163.1(1)	161.6(1)
P(3)–W–P(1)	98.2(1)	98.0(1)
P(3)–W–P(2)	99.4(1)	93.8(1)
C(1)–W–Cl(1)	157.3(3)	
C(2)–W–Cl(1)	156.1(3)	
C(2)–W–C(1)	38.6(4)	
C(2)–C(1)–W	70.2(7)	
C(1)–C(2)–W	71.2(7)	
C(3)–C(1)–C(2)	133.0(11)	
C(9)–C(2)–C(1)	133.3(11)	

* Taken from ref. 16.

[2.019(11), 2.006(11) and 1.330(16) Å respectively] are similar to those found for the tungsten(v) diphenylacetylene complex **3**. The major structural change from complex **3** is the orientation of the diphenylacetylene ligand which now straddles the two *trans* phosphine ligands.

Theoretical Studies.—Hartree–Fock (HF)[18] calculations were carried out on the model complexes $[WCl_5(HC_2H)]^-$ **8** and $[WCl_2(HC_2H)(PH_3)_3]$ **10**, Fig. 4. Scattered wave Xα (SWXα)[19] single-point calculations were performed on the model complexes **8, 10** and the paramagnetic (open-shell) model complex $[WCl_3(HC_2H)(PH_3)_2]$ **9**. The optimised HF internal coordinates of **8** (Table 7), **9** (Table 8) and **10** (Table 9) are in good agreement with the crystal structures. However in complex **10** the calculated C≡C distance and C–C–H angle are slightly overestimated (Table 9). As the molecular orbitals (MOs) produced in the SWXα calculations had very similar characteristics to those from the HF calculations, a general discussion of MO diagrams, population analyses and density plots is appropriate.

Plots of the HF–MO wavefunctions and information from the population analysis show extensive participation from all the carbon p atomic orbitals (AOs) in tungsten–alkyne bonding. The first tungsten–acetylene bonding MO in $[WCl_5(HC_2H)]^-$ **8** [Fig. 5(*a*)] is composed primarily of the HC≡CH($\pi_{\|}$) frontier molecular orbital (FMO), W(d_{z^2}) AO and the terminal Cl(p_z) AO. Thus M–alkyne $\pi_{\|}$ bonding is (in part) well represented by the a_1 (C_{2v} point group) MO in Fig. 1. There exists a corresponding totally antibonding interaction at higher energy, which weakens the W–alkyne bond [Fig. 5(*b*)]. A single MO in which the W(d_{yz})–HC≡CH($\pi_{\perp}$) component is dominant can be identified (Fig. 6) and related to the b_2 MO of Fig. 1. A MO corresponding to the b_1 MO of Fig.1 has been identified in which the filled W(d_{xz}) AO overlaps with the empty HC≡CH($\pi_{\|}$*) FMO in a back-donating interaction [Fig. 7(*a*)].

Table 7 Model structure of $[WCl_5(HC_2H)]^-$ **8**[a]

	X-Ray[b]	SWXα(SP)	HF
W–Cl_t	2.490(3)	2.490	2.461
W–Cl_e	2.365[c]	2.365	2.446
W–alkyne	1.917[d]	1.917	2.005
W–C	2.017[c]	2.017	2.100
C≡C	1.253(14)	1.253	1.251
C–H	—	1.062	1.062
C–C–H	140.3(12)	156.0	156.0
Cl_t–W–Cl_e	84.1[c]	90.0	96.57
Cl_t–W–Cl_e	89.4[c]	90.0	92.19

[a] Cl_t = terminal chlorine ligand, Cl_e = equatorial chlorine ligand. [b] Taken from ref. 14. [c] Average. [d] Calculated from other parameters.

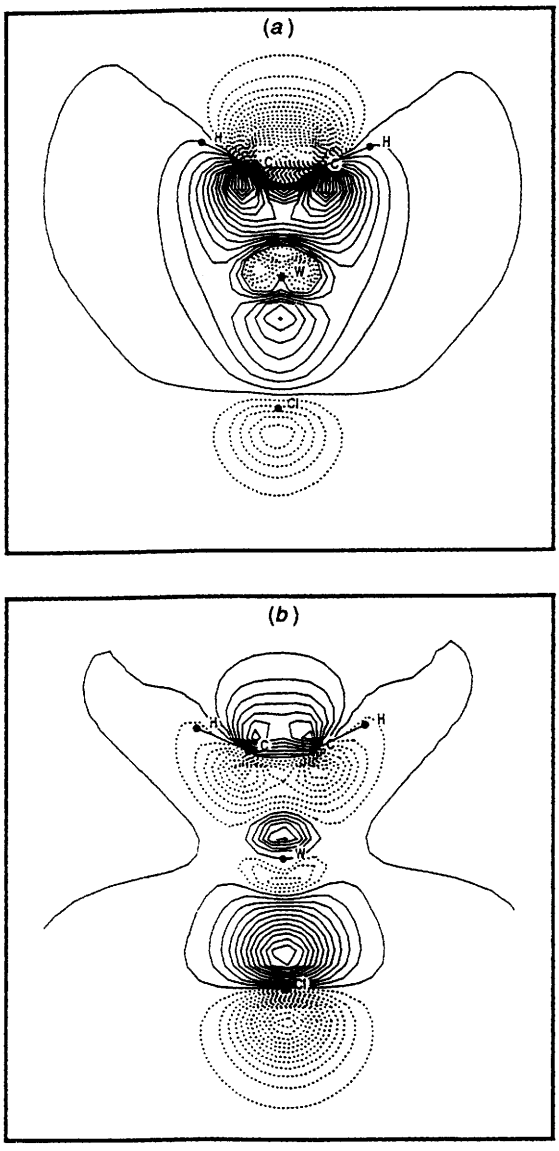

Fig. 5 The W–(HC≡CH) (*a*) σ and (*b*) σ* bonding MO of $[WCl_5(HC_2H)]^-$; MOs in the *xz* plane [contour difference 0.0125, (*a*) max + contour 0.2125, min − contour 0.0875, (*b*) max + contour 0.15, min − contour 0.15]

The highest occupied molecular orbital (HOMO) of complex **8** is composed of W(d_{xz}), HC≡CH($\pi_{\|}$*) and Cl terminal p AO components [Fig. 7(*b*)]. The strong *trans* influence of the acetylene ligand in this complex is demonstrated by the high

Table 8 Model structure of $[WCl_3(HC_2H)(PH_3)_2]$ **9**[a]

	X-Ray[b]	SWXα(SP)
W–Cl_t	2.472(2)	2.472
W–Cl_e	2.400(3)	2.400
W–P	2.565(3)	2.565
W–alkyne	1.929[c]	1.929
W–C	2.030[d]	2.030
C≡C	1.305(11)	1.305
C–H	—	1.062
C–C–H	139.7(9)[d]	156.0
Cl_t–W–Cl_e	84.0[d]	90.0
Cl_t–W–Cl_e	81.0[d]	90.0
Cl_t–W–P	166.6[d]	180.0
P–W–P	161.5[d]	180.0

[a] Cl_t = terminal chlorine ligand, Cl_e = equatorial chlorine ligand. [b] Taken from ref. 4. [c] Calculated from other parameters. [d] Average.

Table 9 Model structure of $[WCl_2(PH_3)_3(HC_2H)]$ **10**[a]

	X-Ray	SWXα(SP)	HF
W–Cl_t	2.500(3)	2.500	2.585
W–Cl_e	2.465(3)	2.465	2.531
W–P	2.481(3)	2.481	2.554
W–P_{trans}	2.539[b]	2.539	2.561
W–alkyne	1.900[c]	1.900	2.252
W–C	2.013[b]	2.013	2.041
C≡C	1.330(16)	1.330	1.455
C–H	—	1.062	1.072
C–C–H(Ph)	133.2[b]	156.0	114.1
Cl_t-W–Cl_e	86.9(1)	90.0	90.8
Cl_t-W–P_{trans}	82.9(1)	90.0	80.6
Cl_t-W–P	76.2(1)	90.0	75.2

[a] Cl_t = terminal chlorine ligand, Cl_e = equatorial chlorine ligand. [b] Average. [c] Calculated from other parameters.

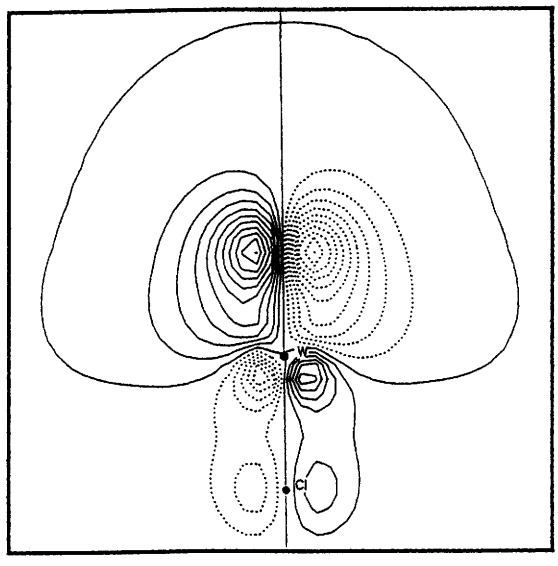

Fig. 6 The W–(HC≡CH) π bonding MO of $[WCl_5(HC_2H)]^-$; MO in the *yz* plane (contour difference 0.0125, max + contour 0.125, min − contour 0.125)

stability of this HOMO, which is antibonding with respect to the terminal W–Cl bond. The lowest unoccupied molecular orbital (LUMO) of complex **8** consists only of the nonbonding W($d_{x^2-y^2}$) AO, thus it appears that the HC≡CH a_2 FMO of Fig. 1 plays no role in W–alkyne bonding. The W($d_{x^2-y^2}$) AO is singly occupied in complex **9** and doubly occupied in complex **10**. In the HOMO energy region there are MOs composed primarily of the other ligand AOs, which may contain some

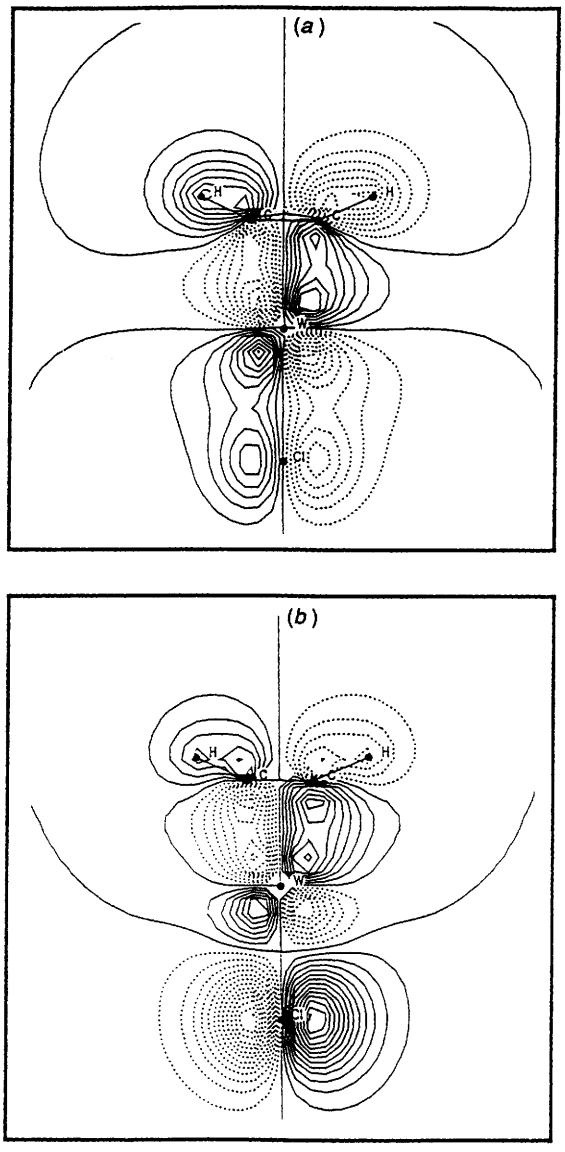

Fig. 7 The W–(HC≡CH) π back bonding MOs of $[WCl_5(HC_2H)]^-$; MOs in the *xz* plane [contour difference 0.0125, (*a*) max + contour 0.1125, min − contour 0.1, (*b*) max + contour 0.1625, min − contour 0.1375)

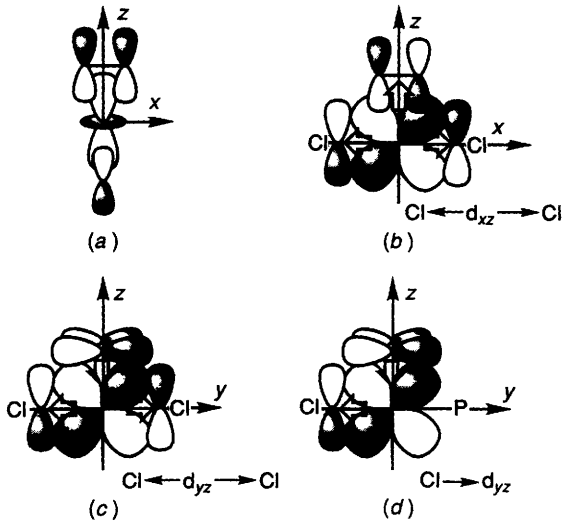

Fig. 8 Qualitative bonding picture for the rotation of the acetylene ligand

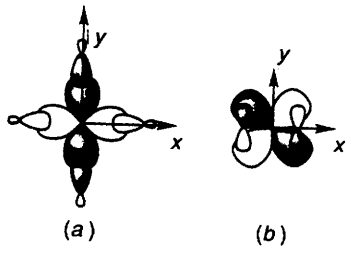

Fig. 9 Representation of the ligand overlap with tungsten; Cl_σ overlap with $W_{d_{x^2-y^2}}$, (*b*) acetylene with $W_{d_{xy}}$ AOs

contribution from the acetylene FMOs and W(d) AOs, but are not important to the tungsten–alkyne bonding.

As noted earlier the acetylene ligand bisects the meridional vectors in $[\{WCl_4(PhC_2Ph)\}_2]$ and $[WCl_3(PhC_2Ph)(PMe_3)_2]$ but *not* in $[WCl_2(PhC_2Ph)(PMe_3)_3]$ (Fig. 4). Molecular orbitals with 'cylindrical' symmetry will not affect the acetylene orientation [Fig. 8(*a*)]. When the acetylene orients along either of the Cl–W–Cl axes in complex **8**, additional electron withdrawal from tungsten towards the more electronegative chlorine atoms *via* a π-type bond occurs, $W(d_{xz}) \longrightarrow Cl(p)$ and $W(d_{yz}) \longrightarrow Cl(p)$, which has a destabilising effect on the tungsten–acetylene bond [Figs. 8(*b*) and 8(*c*)]. Hence, to minimise net withdrawal, the HC≡CH ligand in complex **8** is rotated by 45°. The equatorial Cl ligands now form σ bonds with the $d_{x^2-y^2}$ orbital rather than the d_{xy} orbital [Figs. 9(*a*) and 9(*b*)]. Complex **9** has two phosphine ligands (σ donors only) along one axis, 'replacing' two of the chlorine ligands in **8**. If the acetylene aligns along either axis, Cl–W–Cl or P–W–P, $W(d_{xz}) \longrightarrow Cl(p)$ or $W(d_{yz}) \longrightarrow Cl(p)$, electron withdrawal occurs [Fig. 8(*b*) and 8(*d*)]. To minimise this effect the acetylene is rotated by 56°. This is closer to the P–W–P axis than in complex **8** because of the stabilising $HC{\equiv}CH(\pi_\perp) \longrightarrow W(d_{yz})$ donation [Fig. 8(*d*)]. In complex **10** the $HC{\equiv}CH(\pi_\perp) \longrightarrow W(d_{yz})$ donor interaction and the phosphine ligand (σ donor) contribution are able to compensate totally for the electron withdrawal of the single Cl atom [Fig. 8(*d*) only] and therefore, the acetylene aligns along the P–W–P axis (rotation of 90°).

Population analysis shows that electron density donated through the $HC{\equiv}CH(\pi_{\|})$ FMO to the tungsten increases with the increasing number of Cl ligands (Table 10), as expected from simple electronegativity arguments. The electron density donated through the $HC{\equiv}CH(\pi_\perp)$ FMO should also increase with the increasing number of Cl ligands. However, the donation is greater than expected for complex **9**; this is because the acetylene ligand in complex **9** is rotated 11° more than in complex **8** and as a result the $HC{\equiv}CH(\pi_\perp) \longrightarrow W(d_{yz})$ interaction is enhanced. The total donation of electron density by the acetylene ligands in complexes **8, 9** and **10** well exceeds that donated by the two-electron donor acetylene ligand of the molybdenum complex, $[Mo(C_5H_5)_2(HC_2H)]$, Fig. 10.

The acetylene ligand can compensate the tungsten centre for the effects of other ligands and changes in geometry by altering its acceptance profile (Table 10). In complex **8** there is a shortage of electron density at tungsten and very little back donation occurs. In complexes **9** and **10** the reverse is true. The $HC{\equiv}CH(\pi_\perp{}^*)$ FMO population accepted for complex **9** is small but significant. In complexes **8** and **9** the $HC{\equiv}CH(\pi_\perp{}^*)$ FMO overlaps with the (occupied) $W(d_{xy})$ AO which also overlaps with other ligands [Fig. 9(*a*)]. In contrast the $W(d_{xy})$ of complex **10** does not overlap with other ligands [Fig. 9(*b*)], only the acetylene $HC{\equiv}CH(\pi_\perp{}^*)$ FMO is available for accepting the redistribution of any excess electron density, and therefore the population of this FMO is greater.

The d AO populations also provide insight into the bonding. *d*-Electron density is not localised in a single AO for these

Table 10 Acetylene FMO populations

	Donated			Accepted			
	$\pi_{\|\|}$	$\pi_{\perp}$	Total	$\pi_{\|\|}^*$	$\pi_{\perp}^*$	Total	Net donated
8 $[WCl_5(HC_2H)]^-$	0.700	0.424	1.124	0.272	0.000	0.272	0.852
9 $[WCl_3(HC_2H)(PH_3)_2]$	0.619	0.471	1.091	0.528	0.008	0.536	0.561
10 $[WCl_2(HC_2H)(PH_3)_3]$	0.588	0.358	0.946	0.500	0.055	0.555	0.392
$[Mo(C_5H_5)_2(HC_2H)]$	0.573	0.144	0.717	0.482	0.000	0.482	0.235

Table 11 Tungsten d AO populations

	$d_{z^2}-\pi_{\|\|}$	$d_{xz}-\pi_{\|\|}^*$	$d_{yz}-\pi_{\perp}$	d_{xy}	$d_{x^2-y^2}$	Total d AO
8 $[WCl_5(HC_2H)]^-$	0.263	1.502	0.574	0.797	1.042	4.184
9 $[WCl_3(HC_2H)(PH_3)_2]$	1.050	1.465	0.501	0.602	1.113	4.748
10 $[WCl_2(HC_2H)(PH_3)_3]$	0.628	1.457	0.484	0.772	1.855	5.252

complexes (Table 11). The only formally occupied tungsten d AO is the W(d_{xy}) in complex **10** although the W($d_{x^2-y^2}$) AO is partially occupied in complex **9**.† The W(d_{xz}) AO has a significant population for all of the complexes because it overlaps with the HC≡CH($\pi_{\|}^*$) FMO which lies above the d manifold and shared electrons are found predominantly in the d AO. Formally, however, this AO is considered to be unoccupied because the W(d_{xz})–HC≡CH($\pi_{\|}^*$) bonding MO involves back donation from the tungsten atom to the acetylene ligand. The W($d_{x^2-y^2}$) and W(d_{z^2}) AOs are involved with σ bonding and the population of these d AOs will depend on the nature of the ligands. The population of the W(d_{xy}) non-bonding AO is expected to be approximately constant for all three complexes, however, for complex **9** it is reduced. This is probably due to the W(d_{xy}) AO mixing with the W($d_{x^2-y^2}$) AO as a result of the greater than 45° rotation of the acetylene ligand in this complex.

In complexes **8**, **9** and **10** the acetylene ligand donates significantly more electron density *via* the (HC≡CH)$\pi_{\perp}$ FMO than, for example, the two-electron donor acetylene ligand in the molybdenum complex $[Mo(C_5H_5)_2(HC_2H)]$ (Table 10). The acetylene ligand in complexes **8**, **9** and **10** can therefore be formally denoted as a four-electron donor. Acceptance by the acetylene in the tungsten and molybdenum complexes studied is significant, since there appears to be a fine tuning mechanism operating which is highly dependent on the individual electronic environment each alkyne ligand experiences.[20]

It has been found that the spherically averaged electron density around a specific atom changes in a stepwise manner as the formal oxidation number changes.[21] Orbital population analyses reflect the charge density and therefore the oxidation state of a centre, however, due to the arbitrary nature of partitioning electron density in generating populations the results are relative rather than absolute. For example, the total d AO population of tungsten in WCl_6 is 3.750 e (Fig. 10) which is significantly different from that formally anticipated given the oxidation state of the tungsten is +VI (d^0). Moreover, in the tungsten complexes studied the electron density is highly delocalised, making the assignment of a formal oxidation state to tungsten rather difficult. Comparison of the total d AO population of complexes **8**, **9** and **10** with other relevant complexes is made in Fig. 10. The total d AO population of **8** is very close to that of WCl_6,[4,22] and the populations of complexes **9** and **10** step up from this in a linear relationship. These populations lie well below those for a metal in the +II (d^4) oxidation state. A high-oxidation state formalism is not without precedent for alkyne complexes.[2,6,22,23] The computational results presented lend support to the proposed assignment of formal oxidation states +VI, +V and +IV to complexes related to the model compounds **8**, **9** and **10** respectively.

† Due to rotation of the acetylene in complex **10** the d_{xy} AO is equivalent to the $d_{x^2-y^2}$ AO in complexes **9** and **10** (the axial system was defined with respect to the acetylene). Thus the d_{xy} AO population is reported as the $d_{x^2-y^2}$ for complex **10** and *vice versa*.

Conclusion

The combined results of these studies show that the diphenylacetylene complexes prepared have properties consistent with their formulation as high-valent complexes. The present studies give confirmatory evidence for similar proposals based on previous X-ray structures[6,22,23] and the observed similarity between organoimido and alkyne complexes containing alkyl and alkylidene ligands.[2c] The alkyne ligand stabilises high oxidation states in a manner similar to organoimido and terminal oxo ligands, and thus the oxidation-state formalism is useful when comparing the properties of such complexes.

Experimental

Experimental procedures and instrumentation have been described.[24] Infrared spectra were obtained as Nujol mulls between CsI plates, ^1H and ^{13}C-{^1H} NMR spectra were recorded at 400 and 100 MHz respectively in $CDCl_3$ and EPR spectra were obtained on a Varian E-4 spectrometer operating at 9.5 GHz. Solid-state magnetic moment measurements were made on a Sherwood magnetic susceptibility balance and solution measurements were made at 400 MHz using the Evans' method[25] adapted for a superconducting magnet.[26] X-Ray photoelectron spectra were obtained on an XSAM800 surface analysis instrument. Analytical data were obtained by R. G. Cunninghame and associates, University of Otago, New Zealand. The complex $[\{WCl_4(PhC_2Ph)\}_2]$ was prepared by refluxing WCl_6 and diphenylacetylene in CH_2Cl_2 containing tetrachloroethylene.[5] Trimethylphosphine was prepared by reaction of MgMeI on triphenyl phosphite in dibutyl ether[27] and PMe_2Ph and $PMePh_2$ by reaction of MgMeI on PCl_2Ph or $PClPh_2$. Benzene, toluene and light petroleum (b.p. 40–60 °C) were distilled under nitrogen, from sodium metal, prior to use.

Preparation of the Complexes.—$[WCl_3(PhC_2Ph)(PMe_3)_2]$ **3**. A suspension of $[\{WCl_4(PhC_2Ph)\}_2]$ (3.6 g, 3.58 mmol) in benzene (150 cm^3) was added to sodium–mercury amalgam (Na 0.17g, 7.4 mmol; Hg 45 g) under benzene (50 cm^3) containing PMe_3 (1.6 cm^3, 14.3 mmol) *via* a wide-bore cannula. The mixture was stirred rapidly and shaken frequently over a period of 2 h, filtered and the spent amalgam extracted with benzene (2 × 30 cm^3). The extracts and filtrate were combined and the volatiles removed giving a yellow-orange crystalline solid. Crude yield 3.7 g. The complex was dissolved in toluene (100 cm^3), the solution filtered and crystals obtained by stepwise reduction of the volume. Yield 3.1 g (70%). IR spectrum:

Table 12 Crystallographic data for complexes **3** and **6**

	3	**6**
Formula	$C_{20}H_{28}Cl_3P_2W$	$C_{23}H_{37}Cl_2P_3W$
M	620.60	661.23
Crystal size/mm	0.20 × 0.20 × 0.06	0.12 × 0.09 × 0.04
Crystal system	Orthorhombic	Monoclinic
Space group	$P2_12_12_1$	$P2_1/c$
a/Å	8.378(2)	16.555(3)
b/Å	11.251(2)	9.957(2)
c/Å	25.392(3)	16.889(5)
β/°		103.71(2)
U/Å^3	2393.4(7)	2704.6(11)
Z	4	4
D_c	1.72	1.62
F(000)	1212	1312
μ/cm^{-1}	55.6	48.8
2θ range/°	2–56	2–50
No. of observed reflections	2020 [$I > 3\sigma(I)$]	2673 [$I > 3\sigma(I)$]
A range	0.999–0.759	1.000–0.924
Least-squares weights, w	$1.34/[\sigma^2(F) + 0.000\,64F^2]$	$0.86/[\sigma^2(F) + 0.000\,64F^2]$
No. of variables	237	264
R^a	0.032	0.040
R'^b	0.032	0.041

^{a} $R = \Sigma(|F_o| - |F_c|)^2/\Sigma F_o^2$. ^{b} $R' = [\Sigma w(|F_o| - |F_c|)^2/\Sigma w F_o^2]^{\frac{1}{2}}$.

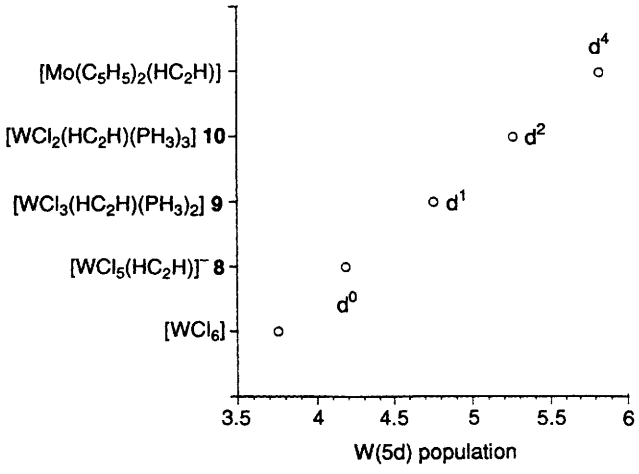

Fig. 10 The W(5d) total AO population

1660w, 1570w, 1460s, 1412s, 1300w, 1270m, 1170w, 1070m, 1022w, 930s, 850m, 775m, 740m, 700s, 680s, 600w, 565w, 518w, 310s, 290s and 260s cm^{-1}.

[$WCl_3(PhC_2Ph)(PMe_2Ph)_2$] **4**. A suspension of [{$WCl_4(PhC_2Ph)$}$_2$] (1.5 g, 1.49 mmol) in benzene (60 cm^3) was added to sodium–mercury amalgam (Na 70 mg, 3.0 mmol; Hg 25 g) under benzene (30 cm^3) containing PMe_2Ph (0.85 cm^3, 6.0 mmol) and stirred rapidly for 30 min as for the preparation of complex **3**. Removal of the volatiles from the combined filtrate and spent amalgam extracts (2 × 10 cm^3) gave an orange-brown crystalline solid. Crude yield 1.8 g. The complex was recrystallised from toluene with stepwise reduction of volume as for complex **3**. Yield 1.5 g (70%). IR spectrum: 1662w, 1460s, 1415s, 1295w, 1270m, 1160w, 1100w, 1075w, 1020w, 1005w, 940s, 905s, 845w, 770m, 738m, 690s, 600w, 565w, 518w, 482m, 415w, 400w, 350w, 310s, 290s and 265s cm^{-1}.

[$WCl_3(PhC_2Ph)(PMePh_2)_2$] **5**. A suspension of [{$WCl_4(PhC_2Ph)$}$_2$] (1.4 g, 1.4 mmol) in benzene (50 cm^3) was reduced with sodium–mercury amalgam (Na 70 mg, 3.0 mmol; Hg 25 g) under benzene (30 cm^3) containing $PMePh_2$ (1.2 cm^3, 6.5 mmol) for 2 h as for complex **3**. The orange crystalline solid obtained on removing the volatiles from the combined filtrate and spent amalgam extracts (2 × 10 cm^3) was recrystallised from toluene as for complex **3**. Yield 1.8 g (75%). IR spectrum: 1664w, 1590w, 1575w, 1480s, 1415s, 1438s, 1400w, 1320w, 1280m, 1275m, 1195w, 1178w, 1160w, 1095m, 1077w, 1025w, 1005w, 938m, 900s, 845w, 775m, 745s, 720s, 710s, 595s, 565w, 500s, 490s, 440m, 310m, 290s and 265s cm^{-1}.

[$WCl_2(PhC_2Ph)(PMe_3)_3$] **6**. A suspension of [{$WCl_4(PhC_2Ph)$}$_2$] (2.0 g, 1.98 mmol) in benzene (50 cm^3) was added to sodium–mercury amalgam (Na 0.2 g, 8.7 mmol; Hg 30 g) under benzene (50 cm^3) containing PMe_3 (1.4 cm^3, 12.7 mmol) *via* a wide-bore cannula. The mixture was stirred rapidly and shaken frequently over a period of 3–4 h, the solution filtered and the spent amalgam extracted with benzene (2 × 30 cm^3). The extracts and filtrate were combined and the solvent reduced to a small volume (*ca.* 10–15 cm^3) giving the complex as green microcrystals. Yield 1.8 g (69%). IR spectrum: 1595m, 1560w, 1420m, 1375m, 1340w, 1295m, 1275m, 1070w, 930s, 850w, 780w, 750w, 720m, 705m, 675m, 600w, 515w, 460w, 350w, 278w and 235s cm^{-1}. NMR: ^{1}H δ 1.52 [d, ^2J(HP) 8.34, 9 H, PMe_3], 1.55 [t, ^2J(HP) 3.88, 18 H, PMe_3], 6.89 [d, ^3J(HH) 7.22, 4 H, *o*-H], 7.11 [t, ^3J(HH) 7.41, 2 H, *p*-H], 7.27 [t, ^3J(HH) 7.71, 4 H, *m*-H]; ^{13}C-{^{1}H} δ 18.58 [t, ^1J(CP) 12.65, PMe_3], 25.98 [d, ^1J(CP) 29.42, PMe_3], 126.07 (*p*-C), 126.12 (*o*-C), 127.74 (*m*-C), 146.58 (*ipso*-C), 223.15 [dt, $^2J(CP_{cis})$ 6.91, $^2J(CP_{trans})$ 15.91 Hz, C≡C].

[$WCl_2(PhC_2Ph)(PMe_2Ph)_3$] **7**. A suspension of [{$WCl_4(PhC_2Ph)$}$_2$] (0.9 g, 0.89 mmol) in benzene (50 cm^3) was reduced with sodium–mercury amalgam (Na 85 mg, 3.7 mmol; Hg 30 g) under benzene (60 cm^3) containing PMe_2Ph (0.80 cm^3, 5.6 mmol) for 3–4 h as for the preparation of complex **6**. Removal of the volatiles from the combined filtrate and spent amalgam extracts (2 × 50 cm^3) gave a yellow-green gum which was allowed to stand under light petroleum for 24 h. Extraction of the solid residue with cold toluene (30 cm^3) left the complex as green crystals. Yield 0.84 g (55%). IR spectrum: 1590m, 1560w, 1470m, 1420m, 1410w, 1290w, 1275m, 1180w, 1160w, 1100m, 1075w, 1028w, 940s, 905s, 840w, 780w, 740m, 695s, 590w, 570w, 490s, 410m, 345w, 325w, 290m and 260m cm^{-1}.

Hydrolysis Reactions of Complexes **1–4**, **6** *and* **7**.—The complex (*ca.* 0.2 g) was suspended in ethanol (20 cm^3) and aqueous sodium hydroxide (*ca.* 20 cm^3, 2 mol dm^{-3}) added. The solution was stirred overnight (or refluxed for several hours if dissolution did not occur), filtered and the volatiles removed. The residue was extracted and dried with anhydrous magnesium sulfate. Removal of volatiles gave an oil which had identical ^{1}H

and ^{13}C-{^{1}H} NMR spectra to an authentic sample of *cis*-stilbene.

Crystallography.—Crystal data for the complexes **3** and **6** are given in Table 12 together with information on instrumentation, data collection and structure determination. Data collection on an Enraf-Nonius CAD-4 diffractometer used graphite-monochromated Mo-Kα radiation (λ = 0.710 69 Å) and ω–2θ scans at variable speed. Lorentz and polarisation corrections were applied using locally written programs and absorption corrections applied from empirical ψ scans. The structures were solved from Patterson and heavy-atom electron-density syntheses and refined by full-matrix least squares on *F* using the program SHELX 76.[29] The heavier atoms were assigned anisotropic thermal parameters, the light atoms were refined isotropically. Hydrogen atoms were included in calculated positions (C–H 0.95 Å) with common isotropic thermal parameters, and allowed to ride on the atom to which they were attached.

Additional material available from the Cambridge Crystallographic Data Centre comprises H-atom coordinates, thermal parameters and remaining bond lengths and angles.

Theoretical Details.—Hartree–Fock (HF) geometry optimisations were performed using GAUSSIAN 90[18] on the model complexes $[WCl_5(HC_2H)]^-$ **8** and $[WCl_2(HC_2H)(PH_3)_3]$ **10** under the restraint of the C_{2v} and C_s point groups respectively, using as initial values data from crystal structures of the complexes, $[PPh_4][WCl_5(PhC_2H)]\cdot CH_2Cl_2$[14] (Table 7) and $[WCl_3(PhC_2Ph)(PMe_2Ph)_2]$ **4** (Table 8). Non-relativistic pseudopotentials and associated basis sets (decontracted) were used for chlorine ([4s4p]/[3s3p]) and phosphorus [4s4p+(1d)]/[3s3p+(1d)],[30] for tungsten a scalar-relativistic pseudopotential and associated basis set ([8s7p6d]/[6s5p3d]) were used.[31] All-electron basis sets were used for C (6–311G)[32a] and H (STO–3G).[32b] Scattered wave Xα (SWXα) single point calculations using the program XASW[19] were carried out on the model complexes **8** and **10**, and the paramagnetic model complex $[WCl_3(HC_2H)(PH_3)_2]$ **9** (Table 8). Bond distances were taken from the associated crystal structures {complex **9** was modelled on $[WCl_2(PhC_2Ph)(PMe_3)_3]$ **6**}. Interatomic angles were chosen to ensure local octahedral symmetry at the tungsten and the C≡C–H angle was set to that from the HF optimisation of **9** (Table 5). Calculations were also carried out on the model complex $[Mo(C_5H_5)_2(HC_2H)]$. Bond distances and angles were taken from the crystal structure[33] of the associated complex $[Mo(C_5H_5)_2(PhC_2Ph)]$ and altered to conform to C_{2v} symmetry. The population analysis of Case and Karplus[34] was applied to the SWXα results. Optimised HF calculations were used to generate the MO diagrams.

Acknowledgements

The support of the University of Auckland Research Committee and the New Zealand Lottery Science Board is gratefully acknowledged.

References

1 J. L. Templeton, in *Advances in Organometallic Chemistry*, eds. F. G. A. Stone and R. West, Academic Press, New York, 1989, vol. 29, p. 1.
2 (*a*) M. D. Curtis, J. Real and D. Kwan, *Organometallics*, 1989, **8**, 1644; (*b*) F. A. Cotton and M. Shang, *Inorg. Chem.*, 1990, **29**, 508; (*c*) K. H. Theopold, S. J. Holms, and R. R. Schrock, *Angew. Chem., Int. Ed. Engl.*, 1983, **22**, 1010.
3 J. B. Hartung and S. F. Pedersen, *J. Am. Chem. Soc.*, 1989, **111**, 5468.
4 A. J. Nielson, P. D. Boyd, G. R. Clark, P. A. Hunt, J. B. Metson, C. E. F. Rickard and P. Schwerdtfeger, *Polyhedron*, 1992, **11**, 1419.
5 E. Hay, F. Weller and K. Dehnicke, *Z. Anorg. Allg. Chem.*, 1984, **514**, 25.
6 S. G. Bott, D. L. Clark, M. L. H. Green and P. Mountford, *J. Chem. Soc., Dalton Trans.*, 1991, 471.
7 C. D. Wagner, W. M. Riggs, L. F. Davis, J. F. Moulder and G. E. Muslenberg, *Handbook of X-Ray Photoelectron Spectroscopy*, Perkin-Elmer, Eden Prairie, St Paul, MN 1979, p. 146.
8 J. Chatt, G. J. Leigh and D. M. P. Mingos, *J. Chem. Soc., A*, 1969, 1674.
9 A. J. Nielson and J. M. Waters, *Aust. J. Chem.*, 1983, **36**, 243
10 W. Levason, C. A. McAuliffe and F. P. McCullough, *Inorg. Chem.*, 1977, **16**, 2911; G. W. A. Fowles and J. L. Frost, *J. Chem. Soc., A*, 1967, 671; D. A. Edwards, G. W. A. Fowles and R. G. Williams, *J. Chem. Soc.*, 1963, 4649.
11 B. Sieklucka, R. Dziembaj and S. Witkowskie, *Inorg. Chim. Acta*, 1991, **187**, 5.
12 D. Brittion, D. W. Macomber and P. G. Gassman, *Acta Crystallogr., Sect. C*, 1982, **11**, 1501.
13 E. Hay, F. Weller and K. Dehnicke, *Z. Anorg. Allg. Chem.*, 1984, **514**, 18.
14 M. Kersting, K. Dehnicke and D. Fenske, *J. Organomet. Chem.*, 1988, **346**, 201.
15 A. Greco, F. Pirinoli and G. Dall'asta, *J. Organomet. Chem.*, 1973, **60**, 115.
16 D. C. Bradley, M. B. Hursthouse, K. M. A. Malik, A. J. Nielson and R. L. Short, *J. Chem. Soc., Dalton Trans.*, 1983, 2651.
17 F. A. Cotton and S. K. Mandal, *Inorg. Chim. Acta*, 1992, **194**, 179.
18 M. J. Frisch, M. Head-Gordon, G. W. Trucks, J. B. Foresman, H. B. Schlegel, K. Raghavachari, M. Robb, J. S. Binkly, C. Ganzales, D. J. DeFrees, D. J. Fox, R. A. Whiteside, R. Seegar, C. F. Melius, J. Baker, R. L. Martin, L. R. Kahn, J. J. P. Stewart, S. Topiol and J. A. Pople, GAUSSIAN 90, Revision J, Gaussian Inc., Pittsburgh, PA, 1990.
19 M. Cook and D. A. Case, Program XASW, version 2, personal communication.
20 D. M. P. Mingos, *Inorg. Chem.*, 1982, **21**, 466.
21 K. Takano, H. Hosoya and S. Iwata, in *Applied Quantum Chemistry*, eds. V. H. Smith, jun., H. Schaefer III and K. Morokuma, Reidel, Dordrecht, 1986, p. 375.
22 R. Stegmann, A. Neuhaus and G. Frenking, *J. Am. Chem. Soc.*, 1993, **115**, 11930.
23 F. A. Cotton and W. T. Hall, *Inorg. Chem.*, 1980, **19**, 2352. F. A. Cotton and W. T. Hall, *Inorg. Chem.*, 1981, **20**, 1285.
24 G. R. Clark, A. J. Nielson, C. E. F. Rickard and D. C. Ware, *J. Chem. Soc., Dalton Trans.*, 1990, 1173.
25 D. F. Evans, *J. Chem. Soc.*, 1959, 2003.
26 D. H. Live and S. I. Chan, *Anal. Chem.*, 1970, **42**, 791.
27 M. L. Luetkens, jun., A. P. Sattelberger, H. H. Murray, J. D. Basil, J. P. Fackler, jun., R. A. Jones and D. E. Heaton, *Inorg. Synth.*, 1990, **28**, 305.
28 A. C. T. North, D. C. Phillips and F. S. Matthews, *Acta. Crystallogr., Sect. A*, 1968, **24**, 351.
29 G. M. Sheldrick, SHELX 76, Program for crystal structure determination, University of Cambridge, 1976.
30 J. C. Barthelat, M. Plessier, P. Villemur, R. Devilliers, G. Trinquier and P. Durand, Program PSHONDO(PSATOM), Toulouse, 1981.
31 D. Andre, U. Häussermann, M. Dolg, H. Stoll and H. Preuss, *Theor. Chim. Acta*, 1990, **77**, 123.
32 (*a*) R. Poirier, R. Kari and I. G. Csizmadia, *The Handbook of Gaussian Basis Sets*, (*a*) Table 6.80.1, p. 263; (*b*) Table 1.15.1, p. 155.
33 A. De Cian, J. Colin, M. Schappacher, L. Ricard and R. Weiss, *J. Am. Chem. Soc.*, 1981, **103**, 1850.
34 D. A. Case and M. Karplus, *Chem. Phys. Lett.*, 1976, **39**, 33.

Received 23rd *September* 1994; *Paper* 4/05797J